محاكاة قدرة الإيقاف الإلكترونية والنووية للأيونات الخفيفة والثقيلة في عنصر السيليكون باستخدام طريقة مونتي كارلو

صالح م. بن صالح، هاجر م. البنغازي، وشريفة م. العرابي
إدارة الفيزياء وعلوم المواد – مركز البحوث النووية
تاجوراء ليبيا

Monte Carlo Simulations of the Electronic and Nuclear Stopping Powers of Light and Heavy Ions in Silicon Material

Saleh M. Ben Saleh, Hajer M. Albangahzi and Shrifa M. Alarabi*
Department of Physics and Material Science
Tajoura Nuclear Research Centre
Tajoura, Libya
* Email: saleh.bsaleh@gmail.com

I. *Abstract*— The stopping power of a material, resulting from the passage of charged particles through it, is an important topic in the fields of applied and industrial sciences. The Stopping power is defined as the amount of energy lost by a particle per unit length of its path through the medium. The process of energy loss for a charged particle passing through the target material must be achieved with high accuracy through direct practical measurements, Monte Carlo simulations or through theoretical calculations. This research provides insight into the stopping powers, projected ranges, longitudinal straggling and lateral straggling of different ions (boron, indium, arsenic, antimony and phosphorus) with energies of 10 KeV to 10 MeV, in silicon target using simulations with the program packages SRIM. In this study, these ions were chosen because they are the most common dopants in the manufacture of silicon semi-conductors. The results of the current study would be used for further research in the field of doping of semiconductor material with light and heavy ions.

Keywords*— *Stopping power, projected Range, straggling, SRIM Software

الملخص

تعد قدرة إيقاف المادة الناتجة عن مرور الجسيمات المشحونة عبرها موضوعًا مهمًا في مجالات العلوم التطبيقية والصناعية. تعرف قدرة الإيقاف على أنها كمية الطاقة التي يفقدها الجسيم لكل وحدة طول من مساره عبر الوسط. يجب أن تتم حساب عملية فقدان الطاقة لجسيم مشحون يمر عبر المادة المستهدفة بدقة عالية من خلال القياسات العملية المباشرة أو محاكاة مونتي كارلو أو من خلال الحسابات النظرية. يقدم هذا البحث نظرة ثاقبة لقوى الإيقاف، والمدى المتوقع، والتشتت الطولي والتشتت الجانبي لأيونات مختلفة (البورون، الإنديوم، الزرنيخ، الأنتيمون والفوسفور) عند طاقات من 10 *KeV* إلى 10 *MeV* في المادة الهدف (السيليكون) باستخدام برنامج المحاكاة *SRIM*. في هذه الدراسة تم اختيار هذه الأيونات لأنها أكثر المنشطات شيوعاً في صناعة أشباه الموصلات السيليكونية. سيتم استخدام نتائج الدراسة الحالية لمزيد من البحث في مجال تطعيم المواد شبه الموصلة بالأيونات الخفيفة والثقيلة.

I. INTRODUCTION

The term stopping power is normally used for charged particles interacting with the target material. Stopping power is a measure of the ability of a material to slow down energetic ions that traverse it [1]. It is defined as the energy loss by charged particles per unit length of a material [2]. The stopping power of ions in different materials is an important quantity and relevant in many application fields such as ion implantation and energy production [3]. Energetic ions penetrating into the target material loss their energy through the interactions with the electrons in the target material (termed as electronic stopping power) and collisions with the nuclei (termed as nuclear stopping power) of the target material. Experimental and theoretical studies devoted to the stopping powers of ions in different materials have been the subject of many researchers for the past few decades.

The stopping powers of ions in a certain material in relevant energy range have been continuously published by many investigators experimentally and theoretically [4-11]. Several computer simulation codes are also available for calculating the stopping powers of ions in matter [11-18]. Among these codes, SRIM (The Stopping and Range of Ions in Matter) is the most widely used software.

SRIM is a software that has been used by many investigators to determine the stopping powers of ions in certain material. The SRIM developed by James F. Ziegler is a collection of programs that use a Monte Carlo method to simulate the interactions of the ions in different target materials [19]. The SRIM software is a freeware and can be downloaded from the following link http://www.srim.org.

This study evaluates the electronic stopping power, the nuclear stopping power, the total stopping power, the projected range, the longitudinal straggling and the lateral straggling of ions (including boron, indium, arsenic, antimony and phosphorus) as they traverse a silicon substrate at energies levels from 10 KeV to 10 MeV, utilizing SRIM Monte Carlo simulation software for analysis.

DOI: **10.5281/zenodo.17075923**

II. SIMULATION METHOD

The SRIM software contains a set of programs that calculate many of the features of ion transport in amorphous material. Figure 1 shows the interface of SRIM package. The software uses the Monte Carlo method, which simulates the transport of ions in matter. SRIM code contains a set of programs that calculate many of the features of ion transport in matter. Applications include the following:

- The SRIM program calculates the energy loss of ions in any material, and includes calculations that produce tables of the stopping power (electronic and nuclear stopping powers), projected range, and straggling distribution for any ion, with any energy. Figure 2 illustrates a screenshot of the SRIM software interface.

- It simulates the process of ion implantation by using ion beams for the purpose of doping them into the substrate in order to modify or change the chemical and electrical properties of the target. It also provides the most important physical phenomena that occur during interactions between the incoming ion beam and the atoms of the target material. Among these phenomena are: ionization of target ions and atoms, creation of holes, phonons, recoiling ions and sputtered atoms. Figure 3 depicts a screenshot of an input setup interface within SRIM program for simulation of ion implantation into amorphous material.

The SRIM code is used in this investigation to perform simulations producing tables of electronic stopping powers, nuclear stopping powers, projected ranges, and energy straggling distributions of boron, indium, arsenic, antimony, and phosphorus ions at energy range from 10 KeV to 10 MeV in a silicon substrate.

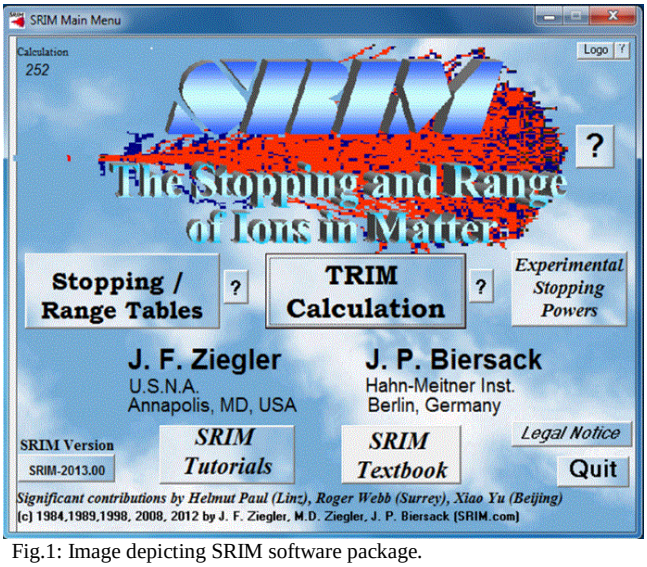

Fig.1: Image depicting SRIM software package.

Fig.2: Application interface included in the SRIM software package for calculating the stopping power of ions in a material. The incident ion is boron and the target is silicon simulated in this study.

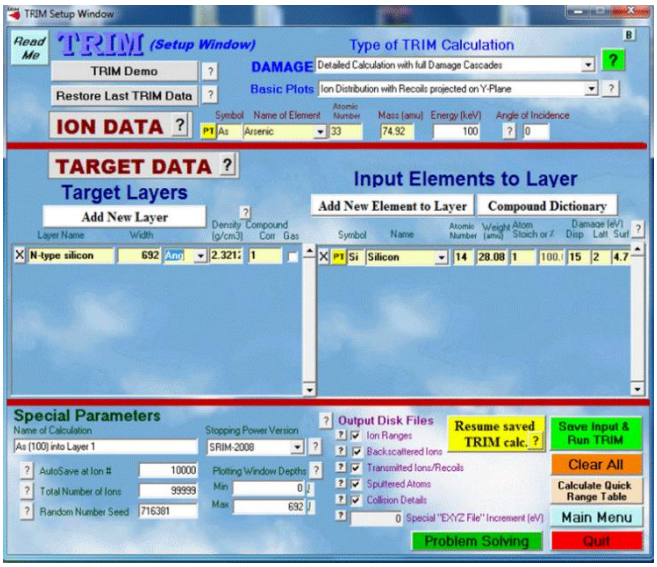

Fig.3: Application interface included in the SRIM software package for simulating ion implantation in amorphous material.

III. PHYSICS FRAMEWORK OF ION ENERGY LOSS IN MATTER

This section discusses briefly the physics and mathematical formulations of ion energy loss in matter. Reference [20] is a key resource in understanding ion stopping power and range calculations, making it an essential reference for specialists in the field.

The total stopping power is defined as the sum of the energy loss components due to nuclear and electronic interactions. It is expressed as [21]:

$$\frac{dE}{dx} = \left(\frac{dE}{dx}\right)_n + \left(\frac{dE}{dx}\right)_e \quad (1)$$

Where E is the ion energy, x is the ion penetration depth, and the subscripts n and e refer to the nuclear and electronic stopping processes, respectively.

As an ion travels through a target material, it loses kinetic energy through interactions with the target's nuclei and electrons. The total stopping power is measured by the stopping cross-section (S), which is simply the sum of its nuclear (S_n) and electronic (S_e) parts. The stopping cross-section is defined as [21]:

$$S = \frac{1}{N}\frac{dE}{dx} = \frac{1}{N}\left[\left(\frac{dE}{dx}\right)_n + \left(\frac{dE}{dx}\right)_e\right] = \frac{S_n + S_e}{N} \quad (2)$$

Where N represents the density of the target material.

When the ion hits a material, it penetrates a certain distance before coming to a stop. This distance is known as the projectile range (R). This stopping distance (depth) is determined by integrating the ion's energy loss from its initial energy (E_0) down to zero [22]:

$$R = \frac{1}{N}\int_0^{E_0}\frac{dE}{S} \quad (3)$$

Nuclear stopping power results from elastic collisions between the incident ions and the target nuclei. A simplified approach, called the binary collision approximation (BCA), focuses on energy transfer between the incident ions and a stationary target atom. Figure 4 describes a schematic representation of a two-body collision. In this model, an incident ion with mass M_1 and initial velocity v_0 collides with a stationary target atom. As a result of the collision: The incident ion is scattered at an angle θ with a new velocity v_1 while the target atom recoils at an angle φ with a velocity v_2. The nuclear stopping cross-section (S_n) quantifies the energy transferred during these elastic collisions, which depends on factors such as the impact parameter p and the transferred energy T_n, as given by equations (4) and (5) [20. 22].

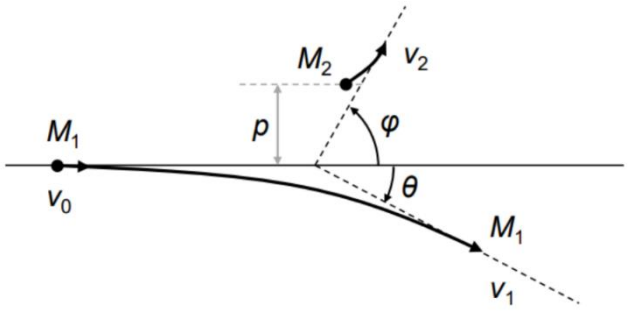

Fig.4: Schematic representation of a two-body collision, adapted from [23]. An incident ion (mass M_1 and velocity v_0) collides with a stationary target, causing the first to be scattered at an angle θ and velocity v_1 and the second (target) to recoil at an angle φ with velocity v_2.

$$S_n = \int_0^{\infty} T_n\, 2\pi p\, dp \quad (4)$$

where T_n is the transferred energy, and p is the impact parameter. the transferred energy is given by:

$$T_n = E\frac{2M_1M_2}{(M_1+M_2)^2}(1-\cos\theta) \quad (5)$$

where E is the initial energy, M_1 and M_2 are the masses of the incident ion and target atom, and θ is the scattering angle.

The energy loss due to electronic stopping is proportional to the velocity of the incoming ion v.The electronic stopping cross-section (S_e) is given by the Lindhard-Scharff model [22,24]:

$$S_e = \frac{8\pi\hbar^3}{m_e e^2}\frac{Z_1^{7/6} Z_2}{\left(Z_1^{2/3}+Z_2^{2/3}\right)^{3/2}}\nu \quad (6)$$

Where m_e is the electron mass, e the elementary charge, Z_1 and Z_2 are the atomic number of the incident ion and the target respectively.

IV. RESULTS AND DISCUSSIONS

In the current research, the calculations were carried out using SRIM Monte Carlo program, which simulates the interactions of ions with matter. The stopping power of ions passing through silicon was computed with energies in the range of 0.01 to 10 MeV. The electronic and nuclear stopping power were calculated in units of (ev / (1E15 atoms/cm2) obtained by SRIM program. There are two mechanisms to stop ions within the target material. One of them is nuclear stopping power that occurs in heavy ions (of high atomic and weight numbers) such as antimony, and the other mechanism is electronic stopping power that occurs in light ions (of low atomic and weight numbers) such as boron. Table 1 gives details of the atomic numbers and atomic weights of the five dopant ions studied. These ions represent the most common dopants in silicon semiconductor manufacturing. The atomic numbers range from boron (lightest at Z=5) to antimony (heaviest at Z=51).

TABLE 1: DETAILS OF THE ATOMIC AND WEIGHT NUMBERS FOR THE IONS USED IN THIS RESEARCH

Ion	Atomic number (Z)	Atomic weight (amu)
Arsenic	33	75
Antimony	51	121
Boron	5	11
Indium	49	115
Phosphorus	15	31

This study presents a dataset on the stopping power, projected range, and energy straggling of five different ions (boron, arsenic, antimony, phosphorus, and indium) implanted into a silicon substrate. The data is organized into tables 2, 3, 4, 5, and 6 for each ion respectively, and covers a range of ion energies from 0.01 MeV to 10 MeV. The results in table (2) indicate that: at low energies (0.01 MeV) the nuclear stopping power of lighter ions (boron) is approximately equal to the electronic stopping power (15.94 vs 18.24), as energy increases, the electronic stopping power mechanism dominates while the nuclear stopping power decreases gradually. Thus, these lighter ions travel deeper into the silicon substrate, resulting in larger projected ranges. At high energies (10 MeV), the electronic stopping power is 161 while the nuclear stopping power drops to 0.1755. The boron projected range at 10 MeV is approximately two orders of magnitude larger than its projected range at 0.01 MeV. The longitudinal and lateral straggling values show the statistical variation in the penetration depth and sideways spread of boron ions respectively, both increase with energy but less dramatically.

Table (3) presents SRIM simulation results for arsenic ions in silicon substrate across energies of 0.01 to 10 MeV. Nuclear stopping power dominates at low energies (< 0.8 MeV) shifting to electronic stopping dominance at higher energies (at 8 MeV: Electronic = 680.1 vs. Nuclear = 33.98). The projected range increases with energy but remains low compared with boron ions. For instance, at 10 MeV, the projected range is 4.08 μm compared to 11.82 μm for boron at the same energy. This is because arsenic (heavy ion) has higher atomic and weight number than boron (light ion) limiting its penetration in the silicon target. The depth variation (longitudinal straggling) and the sideways spread (lateral straggling) both increase with energy exhibiting statistical spread in ion distribution.

TABLE 2: THE STOPPING POWER, PROJECTED RANGE AND ENERGY STRAGGLE DATA FOR BORON IONS IN SILICON SUBSTRATE.

IE(MeV)	S(E) ((ev / (1E^{15} atoms/cm^2))			R_p (μm)	$R_p^{=}$ (μm)	$R_p^{\perp}$ (μm)
	S_e(E)	S_n(E)	S_t(E)			
0.01	18.24	15.94	34.18	0.04	0.0231	0.0173
0.02	25.8	13.1	38.9	0.0771	0.0379	0.0295
0.05	46.05	8.791	54.841	0.1746	0.0642	0.0557
0.06	49.57	7.987	57.557	0.2042	0.0701	0.0622
0.07	52.3	7.337	59.637	0.2332	0.0754	0.0681
0.08	54.53	6.8	61.33	0.2618	0.0802	0.0736
0.09	56.48	6.347	62.827	0.2901	0.0845	0.0788
0.1	58.27	5.958	64.228	0.318	0.0886	0.0837
0.15	66.86	4.617	71.477	0.4519	0.105	0.1047
0.18	72.3	4.095	76.395	0.5271	0.1125	0.1152
0.2	76.05	3.815	79.865	0.5749	0.1169	0.1215
0.25	85.67	3.272	88.942	0.6868	0.126	0.1352
0.3	95.3	2.879	98.179	0.7888	0.1329	0.1464
0.35	104.6	2.578	107.178	0.8824	0.1385	0.1558
0.4	113.5	2.34	115.84	0.969	0.1429	0.1638
0.45	121.7	2.146	123.846	1.05	0.1468	0.1707
0.5	129.4	1.984	131.384	1.13	0.1501	0.1767
0.55	136.4	1.848	138.248	1.2	0.153	0.182
0.6	142.8	1.731	144.531	1.27	0.1555	0.1868
0.65	148.6	1.629	150.229	1.33	0.1577	0.1911
0.7	153.9	1.539	155.439	1.4	0.1597	0.1951
0.8	162.9	1.389	164.289	1.52	0.1636	0.2021
0.9	170.2	1.268	171.468	1.64	0.167	0.2082
1	176	1.168	177.168	1.75	0.1699	0.2137
2	195.3	0.6725	195.9725	2.8	0.1912	0.2511
3	192.8	0.4828	193.2828	3.83	0.2134	0.2774
4	187.6	0.3804	187.9804	4.88	0.2335	0.3004
5	182.3	0.3157	182.6157	5.96	0.2638	0.3219
6	177.4	0.2708	177.6708	7.07	0.2922	0.3426
7	172.9	0.2377	173.1377	8.22	0.3139	0.3628
8	168.7	0.2123	168.9123	9.39	0.3648	0.3828
9	164.8	0.192	164.992	10.59	0.407	0.4027
10	161	0.1755	161.1755	11.82	0.447	0.4226

IE=Ion Energy, S_e(E)=Electronic stopping power, S_n(E)=Nuclear stopping power, S_t(E)=Total stopping power, R_p=Projected range, $R_p^{=}$= Longitudinal straggling, $R_p^{\perp}$= Lateral straggling.

TABLE 3: THE STOPPING POWER, PROJECTED RANGE AND ENERGY STRAGGLE DATA FOR ARSENIC IONS IN SILICON SUBSTRATE.

IE(MeV)	S(E) ((ev / (1E^{15} atoms/cm^2))			R_p (μm)	$R_p^{=}$ (μm)	$R_p^{\perp}$ (μm)
	S_e(E)	S_n(E)	S_t(E)			
0.01	12.83	189.5	202.33	0.0124	0.0047	0.0035
0.02	18.15	219.7	237.85	0.0196	0.0069	0.0053
0.05	28.69	244.3	272.99	0.0388	0.0124	0.0096
0.06	31.43	246	277.43	0.0449	0.0141	0.0109
0.07	33.95	246.4	280.35	0.051	0.0158	0.0122
0.08	36.29	246	282.29	0.0571	0.0174	0.0134
0.09	38.49	245	283.49	0.0631	0.019	0.0146
0.1	40.58	243.6	284.18	0.0692	0.0206	0.0158
0.15	49.76	233.8	283.56	0.0997	0.0282	0.0217
0.18	61.86	227.1	288.96	0.1181	0.0326	0.0251
0.2	66.92	222.6	289.52	0.1303	0.0355	0.0273
0.25	75.04	211.9	286.94	0.161	0.0424	0.0328
0.3	81.28	202.1	283.38	0.1924	0.0491	0.0382
0.35	87.49	193	280.49	0.2243	0.0557	0.0436
0.4	93.86	184.9	278.76	0.2566	0.0622	0.0489
0.45	100.3	177.4	277.7	0.2892	0.0685	0.0542
0.5	106.6	170.6	277.2	0.3221	0.0746	0.0595
0.55	112.8	164.4	277.2	0.3551	0.0806	0.0647
0.6	118.8	158.7	277.5	0.3881	0.0864	0.07
0.65	124.6	153.4	278	0.4213	0.092	0.0751
0.7	130.2	148.6	278.8	0.4544	0.0974	0.0802
0.8	141.1	139.8	280.9	0.5206	0.1079	0.0903
0.9	151.4	132.2	283.6	0.5864	0.1178	0.1001
1	161.3	125.6	286.9	0.6519	0.1271	0.1097
2	251.1	85.71	336.81	1.26	0.1964	0.1906
3	337.2	66.65	403.85	1.79	0.2389	0.2484
4	419.7	55.17	474.87	2.23	0.2659	0.2902
5	496	47.4	543.4	2.62	0.2857	0.3217
6	564.8	41.74	606.54	2.96	0.3001	0.3462
7	626	37.41	663.41	3.27	0.3113	0.3661
8	680.1	33.98	714.08	3.56	0.3215	0.3827
9	727.9	31.18	759.08	3.83	0.3299	0.3969
10	770.2	28.85	799.05	4.08	0.3372	0.4093

Table (4) shows the results for antimony ions (heavies at atomic number = 51), exhibiting an increase in the electronic stopping power at higher energies. The nuclear stopping increases with energy initially (peaks around 0.18 MeV), and

then decreases slightly at higher energies (declines to 86.62 ev at 10 MeV), revealing shorter projected range and smaller energy straggling.

TABLE 4: THE STOPPING POWER, PROJECTED RANGE AND ENERGY STRAGGLE DATA FOR ANTIMONY IONS IN SILICON SUBSTRATE.

IE(MeV)	S(E) ((ev / (1E^{15} atoms/cm^2))			R_p (μm)	$R_p^{=}$ (μm)	$R_p^{\perp}$ (μm)
	S_e(E)	S_n(E)	S_t(E)			
0.01	11.27	240	251.27	0.012	0.0039	0.0029
0.02	15.94	295.7	311.64	0.018	0.0055	0.0042
0.05	25.2	361.5	386.7	0.0326	0.009	0.0072
0.06	27.61	372	399.61	0.0371	0.01	0.008
0.07	29.82	379.9	409.72	0.0414	0.011	0.0089
0.08	31.88	385.9	417.78	0.0457	0.012	0.0097
0.09	33.82	390.4	424.22	0.0499	0.0129	0.0105
0.1	35.65	393.9	429.55	0.054	0.0138	0.0112
0.15	43.66	401.4	445.06	0.0744	0.0182	0.0149
0.18	47.82	401.4	449.22	0.0864	0.0207	0.0169
0.2	50.41	400.3	450.71	0.0944	0.0244	0.0183
0.25	59.6	395.6	455.2	0.1144	0.0256	0.0216
0.3	76.82	389	465.82	0.1341	0.0303	0.0248
0.35	85.35	381.7	467.05	0.1537	0.034	0.028
0.4	90.04	374.1	464.14	0.1733	0.0377	0.0311
0.45	93.35	366.4	459.75	0.1833	0.0413	0.0341
0.5	96.39	358.8	455.19	0.2134	0.045	0.0371
0.55	99.57	351.4	450.97	0.2338	0.0486	0.0401
0.6	103	344.2	447.2	0.2544	0.0522	0.0432
0.65	106.7	337.3	444	0.2753	0.0557	0.0462
0.7	110.5	330.6	441.1	0.2963	0.0592	0.0492
0.8	118.7	318	436.7	0.3388	0.0663	0.0552
0.9	127.1	306.3	433.4	0.3817	0.0732	0.0612
1	135.5	295.6	431.1	0.4251	0.0799	0.0672
2	208.8	222.1	430.9	0.8666	0.139	0.1249
3	267.8	180.9	448.7	1.3	0.1867	0.1771
4	322.2	154.1	476.3	1.72	0.2246	0.2231
5	375.8	135.1	510.9	2.11	0.2563	0.2631
6	429.2	120.8	550	2.48	0.2819	0.2979
7	481.9	109.6	591.5	2.83	0.3029	0.3281
8	533.4	100.5	633.9	3.15	0.3229	0.3545
9	583.2	92.97	676.17	3.45	0.3376	0.3776
10	630.8	86.62	717.42	3.73	0.3511	0.3981

Table (5) shows detailed data for phosphorus ions implanted into a silicon substrate across a range of ion energies. The electronic stopping power starts at 18.2 ev at low energies (0.01 MeV) and increases sharply with energy. The nuclear stopping peaks at 88.57 ev for low energy (0.01 MeV) and rapidly declines with higher energies. The penetration depth (projected range) of phosphorus ions increases with energies from around 0.017 μm at 0.01 MeV up to 4.89 μm at 10 MeV. Also, the energy straggling increases with energy, affecting the uniformity of ion distribution in the substrate. For indium ions shown in table 6, the nuclear stopping dominates at lower energies, shorter penetration depth and small energy straggling variations.

TABLE 5: THE STOPPING POWER, PROJECTED RANGE AND ENERGY STRAGGLE DATA FOR PHOSPHORUS IONS IN SILICON SUBSTRATE.

IE(MeV)	S(E) ((ev / (1E^{15} atoms/cm^2))			R_p (μm)	$R_p^{=}$ (μm)	$R_p^{\perp}$ (μm)
	S_e(E)	S_n(E)	S_t(E)			
0.01	18.2	87.14	105.34	0.0169	0.0083	0.006
0.02	25.73	88.57	114.3	0.03	0.0136	0.0098
0.05	40.69	79.4	120.09	0.069	0.0277	0.0198
0.06	44.57	76.18	120.75	0.0822	0.032	0.023
0.07	50.03	73.17	123.2	0.0954	0.0361	0.0261
0.08	55.42	70.38	125.8	0.1084	0.0399	0.0292
0.09	60.12	67.81	127.93	0.1213	0.0435	0.0322
0.1	64.18	65.44	129.62	0.1342	0.047	0.0351
0.15	78.98	55.95	134.93	0.1979	0.0626	0.0489
0.18	85.48	51.64	137.12	0.2359	0.0709	0.0565
0.2	89.28	49.17	138.45	0.2612	0.0761	0.0615
0.25	97.77	44.06	141.83	0.3242	0.0882	0.0732
0.3	105.7	40.06	145.76	0.3864	0.0989	0.0843
0.35	113.6	36.82	150.42	0.4474	0.1086	0.0947
0.4	121.7	34.13	155.83	0.5069	0.1172	0.1045
0.45	129.9	31.87	161.77	0.5647	0.1251	0.1137
0.5	138.2	29.92	168.12	0.6207	0.1321	0.1223
0.55	146.7	28.23	174.93	0.6749	0.1384	0.1303
0.6	155.2	26.75	181.95	0.7272	0.1441	0.1378
0.65	163.7	25.44	189.14	0.7777	0.1493	0.1448
0.7	172.2	24.27	196.47	0.8266	0.154	0.1514
0.8	188.9	22.26	211.16	0.9194	0.1624	0.1632
0.9	205.3	20.59	225.89	1.01	0.1684	0.1737
1	221	19.19	240.19	1.09	0.1754	0.183
2	343.2	11.78	354.98	1.74	0.2084	0.2404
3	416.3	8.719	425.019	2.24	0.2249	0.2705
4	463.9	7.002	470.902	2.69	0.2356	0.291
5	498	5.889	503.889	3.09	0.2453	0.3068
6	524.2	5.104	529.304	3.48	0.2532	0.3196
7	545.5	4.517	550.017	3.85	0.2599	0.3306
8	563.3	4.06	567.36	4.21	0.2682	0.3402
9	578.5	3.693	582.193	4.55	0.2757	0.3489
10	591.8	3.392	595.192	4.89	0.2825	0.3567

TABLE 6: THE STOPPING POWER, PROJECTED RANGE AND ENERGY STRAGGLE DATA FOR INDIUM IONS IN SILICON SUBSTRATE.

IE(MeV)	S(E) ((ev / (1E^{15} atoms/cm^2))			R_p (µm)	$R_p^{=}$ (µm)	$R_p^{\perp}$ (µm)
	S_e(E)	S_n(E)	S_t(E)			
0.01	11.77	236.2	247.97	0.0119	0.0039	0.003
0.02	16.64	289.3	305.94	0.018	0.0056	0.0043
0.05	26.31	350.7	377.01	0.0329	0.0092	0.0074
0.06	28.82	360.2	389.02	0.0374	0.0103	0.0082
0.07	31.13	367.1	398.23	0.0419	0.0113	0.0091
0.08	33.28	372.3	405.58	0.0463	0.0123	0.0099
0.09	35.3	376.2	411.5	0.0506	0.0133	0.0107
0.1	37.21	379.1	416.31	0.0548	0.0143	0.0115
0.15	45.57	384.2	429.77	0.0758	0.0189	0.0153
0.18	49.92	383.1	433.02	0.0883	0.0215	0.0175
0.2	52.62	381.5	434.12	0.0966	0.0233	0.0189
0.25	62.74	375.7	438.44	0.1173	0.0275	0.0224
0.3	73.11	368.4	441.51	0.1379	0.0316	0.0257
0.35	79.58	360.5	440.08	0.1586	0.0357	0.0291
0.4	84.63	352.5	437.13	0.1794	0.0396	0.0323
0.45	89.36	344.5	433.86	0.2005	0.0435	0.0356
0.5	94.11	336.8	430.91	0.2218	0.0474	0.0388
0.55	98.94	329.3	428.24	0.2432	0.0513	0.042
0.6	103.8	322	425.8	0.2649	0.0551	0.0452
0.65	108.7	315.1	423.8	0.2867	0.0588	0.0484
0.7	113.5	308.5	422	0.3086	0.0625	0.0516
0.8	122.8	296	418.8	0.3529	0.0699	0.058
0.9	131.7	284.6	416.3	0.3976	0.0771	0.0643
1	140.1	274.2	414.3	0.4427	0.0841	0.0706
2	209	203.8	412.8	0.903	0.1454	0.1311
3	270	165.1	435.1	1.36	0.1944	0.1854
4	331.1	140.2	471.3	1.78	0.2332	0.2324
5	392.4	122.6	515	2.18	0.2629	0.2723
6	452.8	109.4	562.2	2.54	0.287	0.3062
7	511.1	99.11	610.21	2.87	0.3063	0.335
8	566.5	90.79	657.29	3.18	0.3235	0.3598
9	618.6	83.92	702.52	3.47	0.3379	0.3815
10	667.4	78.13	745.53	3.75	0.3501	0.4005

Figure 5 displays the results from SRIM simulation of boron ions in a silicon target over a wide energy range. It explains the variation of the electronic and nuclear stopping powers with boron energy. It shows that the electronic stopping is the main energy loss mechanism, reaching a peak around 2.75 MeV, enabling deeper penetration of boron ions into the silicon substrate. The nuclear stopping power starts higher at low energy (0.01 MeV), but becomes less significant as energy increases.

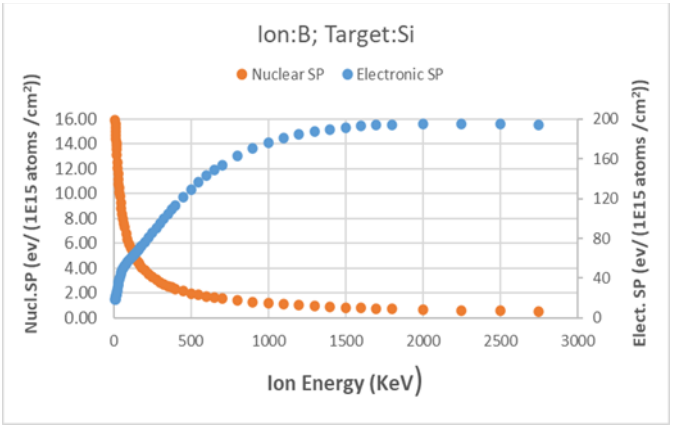

Fig.5: Electronic and nuclear stopping power as a function of ion energy for boron.

Figure 6 describes the behavior of energy loss of arsenic ions in silicon. we distinguish several seniors: at lower energies, the nuclear stopping resulting from elastic collisions between the ion and the target atoms is dominant, it reaches a maximum of about 70 KeV, which corresponds to an energy loss of approximately 246.4 (ev / 1E^{15} atoms/cm^2). At an energy interval of 800 KeV, arsenic ions are suppressed by both the nuclear and electronic energy loss mechanisms. When the energy exceeds 800 KeV, the stopping power of electronic mechanism becomes dominant compared to nuclear stopping power. This electronic mechanism expresses the inelastic interaction between the ions and the orbital electrons of the target atoms and is responsible for excitation and ionization of the target atoms.

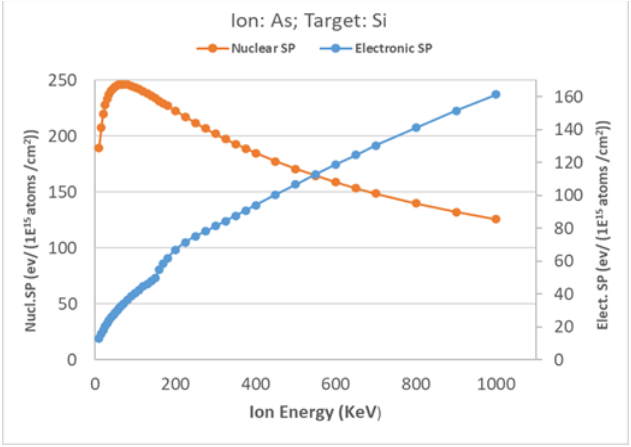

Fig 6: Simulating the nuclear and electronic stopping power of arsenic ions in the silicon target in terms of the incident energy of the ions.

Figure 7 describes how both the electronic and nuclear stopping powers of antimony ions vary with incident ion energy as they traverse a silicon substrate. The nuclear stopping power (orange curve) initially rises sharply at low energy (around 180 KeV), then starts to decrease as the energy increase further. The electronic stopping power mechanism (blue curve) starts relatively low at lower

energies but increases gradually with energy. Beyond the crossing point near 2 MeV, it becomes the dominant energy loss mechanism.

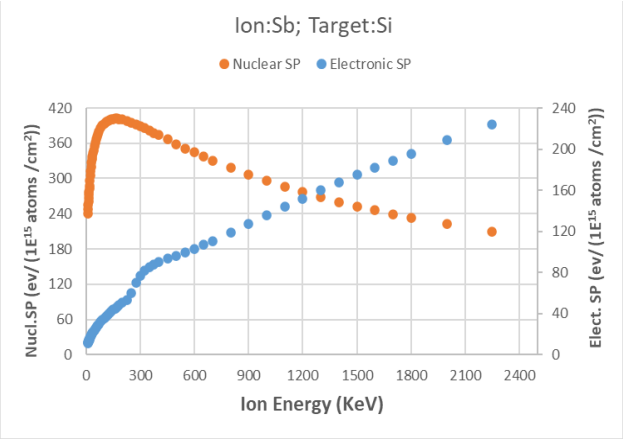

Fig. 7: Electronic and nuclear stopping power as a function of ion energy for antimony.

V. Conclusion

According to the current study on the issues of stopping powers, projected range, and energy straggling of five different ions traversing a silicon substrate, we may conclude some important points as follows:

- Light ions (boron, phosphorus), the electronic stopping power is the dominant energy lose mechanism (interactions with electrons), and penetrate deeper into the silicon substrate.

- Heavy ions (antimony, indium, and arsenic), lose energy via the nuclear stopping mechanism (collision with nuclei) especially at low energies and exhibit shallower projected range compared with lighter ions.

- The longitudinal and lateral straggling increase with energy, resulting in a noticeable statistical variation in ion trajectories at higher energies.

- Heavier ions show smaller energy straggling compared with lighter ions, as they are less deflected by collisions with the target material.

References

[1] Correa, "Calculating electronic stopping power in materials from first principles". *Computational Materials Science* Vol. 150, Pages 291-303, July 2018.

[2] Khan, Faiz M. The physics of radiation therapy 3rd edition. Lippincott Williams & Wilkins, p113, 2003.

[3] H. Hieslmair, L. Mandrell, I. Latchford, M. Chun, J. Sullivan, B. Adibi, "High Throughput Ion-Implantation for Silicon Solar Cells". *Energy Procedia* 27, pages 122 – 128, 2012.

[4] Ziegler, J.; Biersack, J.; Ziegler, M., SRIM The stopping and range of ions in matter. Lulu Press: Morrisvil, 2008.

[5] Bichsel, H., *Stopping power of fast charged particles in heavy elements: National Institute of Standards and Technology*, Gaithersburg, MD, Report NIST IR 4550, 1991.

[6] Sand, R. Ullah and A. Correa. "Heavy ion ranges from first-principles electron dynamics". npj Computational Materials (2019) 5:43

[7] Sigmund, P. "Stopping power in perspective". *Nucl. Instrum. Methods Phys.* Res. B 135, 1–15, 1998.

[8] Correa, A. A. "Calculating electronic stopping power in materials from first principles". *Comput. Mater. Sci*. 150, 291–303, 2018.

[9] M. Msimanga, C.M. Comrie, C.A. Pineda-Vargas and S. Murray. "Experimental stopping powers of Al, Mg, F and O ions in ZrO2 in the 0.1–0.6 MeV/u energy range". *Nuclear Instruments and Methods in Physics Research* B 268, 1772–1775, 2010.

[10] Ziegler, J.F., Ziegler, M.D., Biersack, J.P., SRIM — the stopping and range of ions in matter (2010), *Nucl. Instrum. Methods Phys*. Res. B 268, 1818–1823, 2010.

[11] Francesc Salvat, "Bethe stopping-power formula and its corrections". *PHYSICAL REVIEW* A 106, 2022.

[12] Ziegler, J.F., Biersack, J.P., Littmark, U., the Stopping and Range of Ions in Solids, Pergamon Press, New York, 1985.

[13] International Commission on Radiation Units and Measurements, Stopping Powers and Ranges for Protons and Alpha Particles, ICRU Report 49, ICRU, Bethesda, MD, 1993.

[14] Paul, H., Schinner, A., An empirical approach to the stopping power of solids and gases for ions from 3Li to 18Ar, *Nucl. Instrum. Methods Phys.* Res. B 179, 299–315, 2001.

[15] Paul, H., Schinner, A., An empirical approach to the stopping power of solids and gases for ions from 3Li to 18Ar: *Part II, Nucl. Instrum. Methods Phys*. Res. B 195, 166–174, 2002.

[16] Geissel, H., Weick, H., Scheidenberger, C., Bimbot, R., Gardès, D., Experimental studies of heavy-ion slowing down in matter, *Nucl. Instrum. Methods Phys.* Res. B 195, 3–54, 2002.

[17] Agostinelli, S., et al., Geant4 — A simulation toolkit, *Nucl. Instrum. Methods Phys*. Res. A 506, 250–303, 2003.

[18] Allison, J., et al., Geant4 developments and applications, *IEEE Trans. Nucl*. Sci. 53, 270–278, 2006.

[19] J. F. Ziegler, SRIM Software version 2013.00 from http://www.srim.org.

[20] J. F. Ziegler, "The stopping and range of ions in solids," in Ion Implantation Science and Technology (Second Edition), Academic Press, 1988.

[21] J. F. Ziegler, J. P. Biersack, and M. D. Ziegler, SRIM: The Stopping and Range of Ions in Matter. 2015.

[22] M. Janson, "Hydrogen diffusion and ion implantation in silicon carbide", PhD Thesis, KTH Stockholm, 2003.

[23] J. M¨uting, "Impact of dopant distribution on sic power mosfets,", Ph.D. dissertation, ETH Zurich, Zurich, 2019

[24] J. Lindhard and M. Scharff, "Energy dissipation by ions in the keV region", *Physical Review*, vol. 124, no. 1, 1961.